

Ti6Al4V-AA1050-AA2519 explosively-cladded plates under impact loading

T. Frasn^{1,a}, I. Szachogluchowicz², and L. Sniezek²

¹ French-German Research Institute of Saint-Louis (ISL), 5 rue du Général Cassagnou, 68301 Saint-Louis, France

² Military University of Technology (WAT), ul. gen. S. Kaliskiego 2, 00-908 Warsaw, Poland

Received 6 November 2017 / Received in final form 19 April 2018
Published online 10 september 2018

Abstract. The aim of the study is to analyse perforation processes in explosively-cladded Ti6Al4V-AA1050-AA2519 plates impacted by fragment-simulating projectiles at velocity 500–750 m/s. A high strength titanium alloy is the striking face and a ductile aluminium alloy is the underlying, backing layer. The explosive welding may be an optimal technique of bonding of these two dissimilar metals without affecting their mechanical properties in a composite armour plate. The experimental observations of the plates deformation and failure are completed by a FEM simulation and a SEM fractography to analyse behaviour of such a layered metallic composite under impact loadings.

1 Introduction

Explosive cladding is a welding process in which due to a controlled explosive detonation, sheet metals, non-weldable by conventional methods, are bonded [1]. Surfaces of the parent metals are not melted but plasticized to create a high-quality metallurgical bond. The bonding is a transition from the clad metal to the base metal with no degradation of their physical or mechanical properties (e.g. [2,3]). The technique was initially used to manufacture multi-layered combinations of metals with enhanced properties for aviation and space applications. In particular, titanium-aluminium explosively-cladded plates have been proposed as shields against impacts of space debris. Each layer plays a specific role in a complete behaviour of a layered composite. Titanium, as the striking face is characterized by a high strength required shatter projectiles and to dissipate their impact energy. Aluminium, as the backing layer is ductile enough to capture fragments and debris. Resulted structures are characterized by a high strength and regarding a protection level, not so high weight. Similar concepts are in the basis of the amour development.

Various properties of titanium-aluminium explosively-cladded plates have been discussed in literature (e.g. [4–6]). There are also publications which refer to the same explosively-cladded AA2519-AA1050-Ti6Al4V laminates, which have been tested for needs of the hereby presented study [7–12]. Boronski et al. [7] and Bazarnik et al. [8] describe the mechanical properties of the cladded plates at ambient temperature

^a e-mail: teresa.fras@isl.eu

and in cryogenic conditions. Szachogluchowicz et al. [9,10] focus on the composite behaviour under low- and high-cycle fatigue tests. These works present also more information and details of the conducted manufacturing process.

A number of papers describes protective properties of various laminated targets under impacts of different ballistic threats. However, most of publications is focused on multi-layers targets manufactured in a traditional way (connected by screws, e.g. [13], or by adhesive bonding, e.g. [14]). Studies on behaviour of explosively-welded amours under impact loadings, as well as their numerical analyses are rare. To the best knowledge of the authors, only a research team, which published [15] as one of first papers in this topic, discusses ballistic experiments and their numerical simulations to analyse the performance of explosively welded steel/aluminium plates. Numerical studies on the process of explosive welding itself are more popular, e.g [16,17]. Efforts are devoted to simulate the explosion, its physical parameters and to determine variables of the welding process and their influence on the bonding. In that case, also different numerical techniques are adopted, like the traditional Lagrangian FEM approach [16], or the smoothed-particle hydrodynamics (SPH) method [17].

The presented paper discusses properties of the explosively-cladded Ti6Al4V-AA1050-AA2519 plates considered as an armour against kinetic threats. In the performed investigation, fragment-simulating projectiles (FSPs) were shot. The microstructure of perforation zone is depicted in the SEM images to analyse fracture modes occurred in the subsequent plate layers. The experimental observations are completed by the numerical analysis carried out in the Lagrangian finite element explicit code Ls-Dyna. Mechanisms of penetration and perforation are investigated aiming to understand how explosively-welded layered structures behave under impact loadings.

2 Material description

Due to explosive welding of parallel plates, in a single, laminated plate, properties of titanium and aluminium alloys were enhanced along the plate thickness. The base layer was a 10 mm thick Ti6Al4V alloy sheet and the overlaid layers were a 10 mm thick AA2519 alloy sheet and an approximately 0.5 mm thick unilaterally rolled sheet of the AA1050 aluminium. Quality of bonds depends on a control of process parameters, such as surface preparation, plate separation, detonation energy and detonation velocity. Figure 1b depicts the measurements of micro-hardness in the connection zone proving that initial properties of the bonded materials were not much affected by the welding process. Details of the applied welding technology are presented in [11,12].

The titanium alloy has a structure consisting of coarse grains rich in vanadium, as well as aluminium precipitations located at grain borders. Following [9,10], it is assumed that the alloy is characterized by the tensile strength of 1050 MPa and a 14% elongation. The AA2519 aluminium alloy (AlCuMgMn +a ZrSc added to improve ductility) is characterized by a good plasticity and a relatively high strength – the tensile strength equals to 335 MPa and the elongation reaches 17% [8]. Because an additional thin layer is required as a technological spacer (interlayer) to reduce a potential brittleness of the intermediate Al-Ti zone created by the welding, an aluminium with different properties was chosen as the interlayer. The aluminium AA1050 has the tensile strength of 105 MPa and is characterized by the elongation close to 12%.

During the cohesion of metals in the contact zone, high-intensity narrowly-localized plastic strains occur mostly in a wave-shape. The low strength AA1050 thin

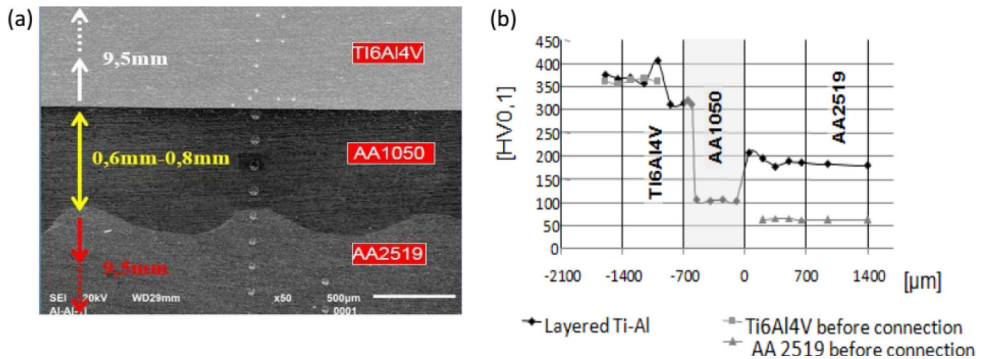


Fig. 1. (a) The connection resulted from the explosive welding (AA2519-AA1050 interface – in a form of waves and the flat Ti6Al4V-AA1050 interface) and (b) changes in the microhardness in the connection zone [10].

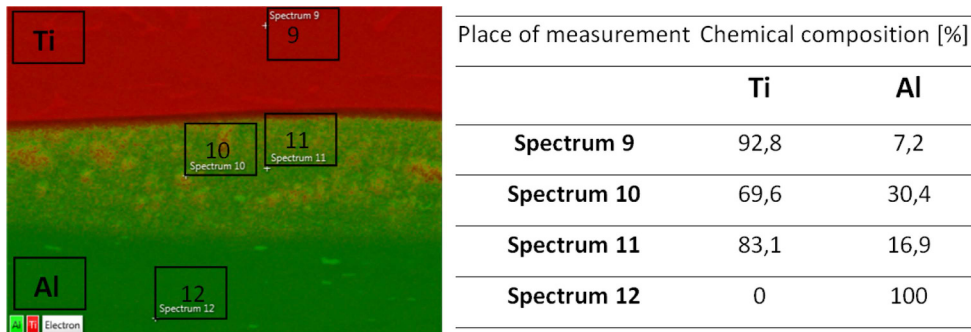


Fig. 2. The EDS chemical analysis of the Ti6Al4V-AA1050 interface.

layer was applied as the binder, the connection between the AA1050 and AA2519 layers has a corrugated interface and the Ti6Al4V-AA1050 interface is flat (Fig. 1a).

Analysis of the interfaces reveals a complex structure which consists of a few successive hierarchical levels with a deformation gradients in both parent materials. Mesoscopic scale shows a wavy Al-Al interface resulted from an expansion of plastic shear waves during the explosion. At a microscopic regime, the intermetallic zone with inclusions is observed in the Ti6Al4V-AA1050 bonding. An energy-dispersive X-ray spectroscopic (EDS) analysis revealed a sub-layer of a width 3–40 μm , within which Al_3Ti or Ti_3Al intermetallic precipitates occur (Fig. 2).

Occurrence of intermetallic inclusions is confirmed also by other studies [18–20], where it is confirmed that intermetallics occur in a properly developed bond. Inclusions may contain micro-cracks that did not expand into the bulk materials. In [19], it is proved that the shear strengths of the joints with dissimilar welding parameters show a pronounced dependency on the formation of intermetallics. Susceptibility of brittle intermetallics for cracking may result in a potential weakness of joints. Lower constituent of intermetallic reactions on the interface increases its strength. At the lowest hierarchy level, a 100–300 nm thick layer of nanocrystals may be noticed (see also [19] and Fig. 5.2). Additionally, in the bonding zone a compensation of residual stresses (remained after the explosive welding processes and not relieved afterwards) may influence the strength of joints [10].

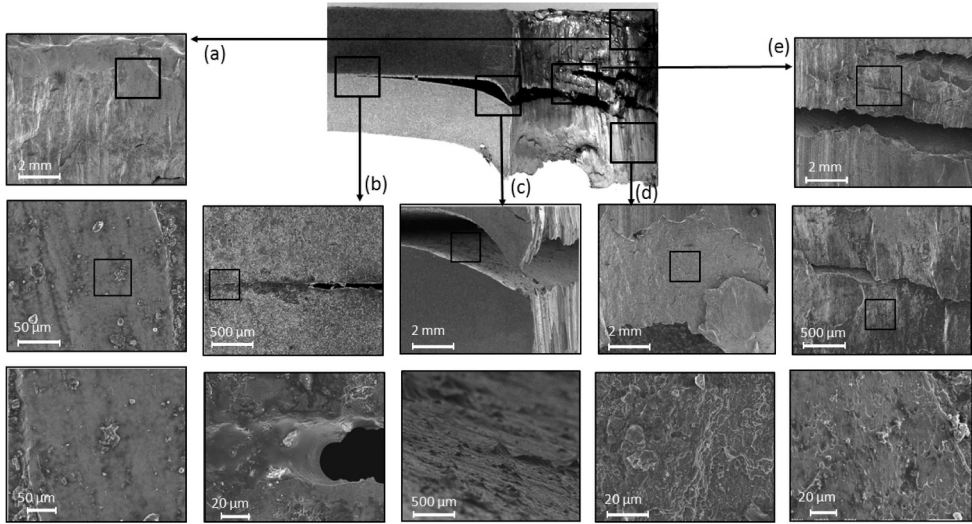


Fig. 3. Details of the perforation channel under a scanning microscope. Impact velocity equals to 647 m/s.




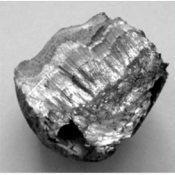


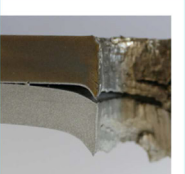




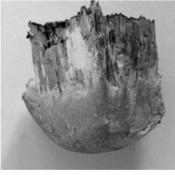
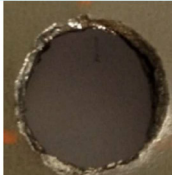



3 Ballistic impact test

Fragment-simulating projectiles are the reference penetrators used to simulate artillery shell fragments [21]. Their shape is non-axisymmetric and the dimensions and material properties fulfil requirements of military specifications [22]. A FSP has a flat, chiselled nose at the angle of 35° . With 20 mm diameter and weight of 53.8 g, it represents a 155 mm artillery shell fragment [21]. It consists of an AISI 4340-H steel alloy, heat-treated to a hardness of HRC 30. Ballistic impact test with FSPs is mandatory for the evaluation of protection levels in the component acceptance tests.

To a shot, each plate of the size $250 \times 250 \times 20$ mm was stabilized in a steel frame. FPSs were accelerated by a powder gun. The impact velocity was measured by a pair of light-barriers. The impact yaw and pitch angle as well as the projectile's residual velocity after a target perforation were obtained due to a triple-exposure flash X-ray device. It was checked that at the impact moment, projectiles were perpendicular to the plate.

In Table 1, some features of the impact zones and perforation channels are presented. Impacts with higher velocities caused a larger deformation of the plates and a more distinct delamination between aluminium layers. With higher impact velocities, the entry holes, as well as the penetration channels and exit holes had higher diameters. All plates were perforated in a similar manner. The global deformation mode changed from a ductile hole enlargement, through a mechanism of highly localized shear around the projectile nose, to the final plugging. Plug is a part of metallic material of a specific shape, which is sheared out from a target plate by a deforming projectile [23,24]. In each case, the plate perforation was followed by a delamination between the interfaces of AA2519 and AA1050. Rupture on the border between the interfaces of Ti6Al4V and AA1050 is not observed. Since no similar studies on the dynamic failure of Ti6Al4V-AA1050-AA2519 panels have been carried out, it cannot be stated if debonding between the corrugated aluminium interfaces is typical for these structures. In [15], other metals pairs have been clad explosively (steels and aluminium) and no interlayers (a technological spacer, like AA1050 in the discussed case) was added during the manufacturing process.

Table 1. Features of the perforation zones.

Impact velocity [m/s]	Residual velocity [m/s]	Entry hole (in Ti6Al4V) Dimensions in two directions [mm]	Exit hole (in AA2519) Dimensions in two directions [mm]	Cross-section	Plug
756	348	 25.5 x 24.4	 31.5 x 34.8		
647	247	 24.1 x 22.8	 26.6 x 23.2		
576	150	 22.15x21.50	 25.8 x 22.7		
510	107	 22.2x22.50	 25.2x 22.1		

In the subsequent target layers, below the projectile, on its periphery, shearing occurred which led to the separation of the plug. This is a dominant failure mode noticed directly after the impact. In Figure 3, the SEM images of the titanium and aluminium (the pictures sequence “d” – for AA2519, “a” and “e” for Ti6Al4V) depict smooth surfaces, which confirms the ductile shearing as a dominant process leading to perforation. The “c” group of SEM images depicts smooth surfaces with some ductile “cones” on the AA2519 upper face. The magnifications show regions with a partly melted structure (both in the titanium and aluminium layers) and the areas covered by typical ductile dimples observed on sheared surfaces of ductile materials. Thermal changes of the structure may indicate that it underwent a fast adiabatic transformation.

In the titanium plate (pictures “e”), some delaminations between internal structural layers (those resulted from the initial rolling manufacturing processes) are

observed. They are close to the rear side of the plate, in a region deformed in the shape of a bulge, where the bending of the titanium layer was the largest. The titanium and aluminium interfaces are not deformed in the same manner, the bottom titanium face is more “curved” comparing to the upper aluminium surface, which is more smoothly bended. It may mean that the deforming AA2519 aluminium plate was separated from the upper Ti-Al layers before the projectile passed through the titanium layer.

The cross-sections of the samples revealed debonding in the AA1050 aluminium. During the penetration, the moving projectile pushed the structure directly below its nose, which caused stretching of the target layers. In Table 1, it may be seen that on the rear plate face (bottom side of the AA2519 layer), a ductile bulge was formed before the plug was ejected. The deformation of the ductile backing layer was larger than this of the thinner and weaker AA1050 layer. A magnification of the beginning of discontinuity (the set “b”) in the bonding reveals a smoothly deformed structure. Figures 1a and 3b show that the connection between the aluminiums was properly developed and is of a high quality. The “wavy bonding” is obtained only if conditions of the explosion are properly chosen and the welding process is conducted without errors. The undamaged faces of both aluminiums in the zone of bonding also prove that observation. The breakage in the welding joint is not a result of coalescence of its internal discontinuities but of a mechanical loading due to which tensile forces caused an extensive stretching leading to rupture.

Assumptions about dynamic processes are built basing on the analysis of microscopic images of the structure already fractured. Such “post-mortem” conclusions must cause some uncertainties. Usually, they may be confronted with their numerical simulation. Challenges in numerical modelling of impacts into explosively-welded structures are presented in the next section.

4 Preliminary numerical simulation

Among several issues which must be considered in a numerical modelling of impact events (e.g., characterization of deformation and fracture of involved materials, proper simplifications to optimize time of calculations, influence of mesh size on results, properly chosen boundary conditions, optimal numerical technique), simulations of impacts in explosively-cladded plates accounts for one more challenge – modelling of the interfaces and the contact between them. As it was presented in Section 2, the structure of a metallurgical bonding is complex and often has unknown properties.

Basing on the examples found in literature [15], the contact between interlayers was modelled using the Ls-Dyna option *TIEBREAK_SURFACE_TO_SURFACE [25]. The tie-break contact models a connection which transmits both compressive and tensile forces with a failure criterion (traditional contacts transmit only compressive forces without failure).

The tie-break contacts have an additional feature; they include a failure criterion indicating the contact breakage:

$$\left(\frac{|\sigma_n|}{\text{NFLS}} \right)^2 + \left(\frac{|\sigma_s|}{\text{SFLS}} \right)^2 \geq 1, \quad (1)$$

where NFLS denotes the tensile failure stress and SFLS is the shear failure stress [25]. The criterion does not account for a temperature influence.

If the condition (1) exceeds 1, nodes are not connected any more. The separation of the slave node from the master node is resisted by a linear contact spring for both tensile and compressive forces until the failure, after which the tensile coupling is

removed [25]. By this function, the physical breakage of the interfacial bonding may be modelled if stresses acting on the interfaces are greater than forces connecting them. Values of the failure stresses NFLS and SFLS are not physically characterized, they may differ depending on the impact configuration. In [15], no discussion on dependence between these parameters and simulated debondings is provided.

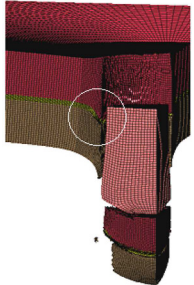

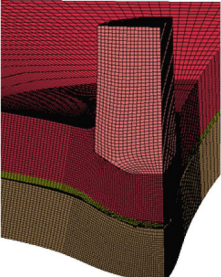
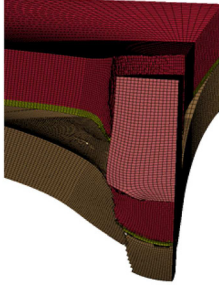
A fine mesh (elements of size 0.2 mm) was applied in the impact zone of a quarter of the modelled plate. The element size increases gradually reaching 1.5 mm on the outer edge, which resulted in a total number of 450 000 elements. Boundary constraints were applied to the planes of symmetry of the target layers and their side faces were constrained. The contact algorithm *ERODING_SURFACE_TO_SURFACE was chosen to describe interactions between the projectile and the target allowing for a crack growth during the perforation process. In the preliminary simulation, to verify the tie-break contact condition, both interfaces Ti-Al and Al-Al were assumed as having same geometrical conditions, so they are flat. The “wavy” shape of the connection between the aluminium layers was not modelled. This simplification reduced a number of elements (to model properly a single wave period with the amplitude 0.1–0.2 mm and length 0.6–0.8 mm, elements would have a maximal size of 0.05 mm resulting in 2 elements in the wave amplitude) and optimized the time of calculations. In a continuation of the numerical study, this problem as well as some other issues (like a better characterisation of mechanical properties of the metals and a more profound study on contact functions) should be improved.

The Johnson and Cook plasticity and fracture models were chosen to describe the deformation and fracture of the titanium and aluminium alloys [26,27]. Both functions account for the strain rate and temperature in description of the plasticity and fracture strain. Their simplicity and efficiency in predictions of behaviour of steels and metals under different loadings is well known and proven by a hundreds publications (e.g. [13,23]). The constitutive relations were implemented in Ls-Dyna as *MAT_MODIFIED_JOHNSON_COOK (*MAT_107) [28]. This implementation of the JC models does not require the equation of state and a series of publications (e.g. works of Borvik and co-authors) shows that simulations with *MAT_107 give good results, (e.g. [13,23,28,29]).

All models parameters are taken from published studies. Because of the approximation of the material behaviour by the model parameters taken from the literature, some limitations are imposed to the numerical modelling. Even more difficult in a numerical analysis of the perforation of clad structures is characterisation of the contact between layers. Regarding the Ti6Al4V alloy, four different sets of parameters may be found in [30], another set quoted after [31] was used in the presented simulation. The parameters describing an aluminium of the series 2xxx (AA2024) were also taken from this publication because of a lack of data describing the alloy AA2519. Studies on AA1050 are not advanced either; some basic data about the behaviour of the alloy in dynamic conditions are presented in [32]. Because of a lack of other data, for both aluminiums the same values of D_1 – D_5 parameters were assumed, which allowed to gain a first insight on the influence of temperature and strain rates on their deformation and failure. The melting temperature and the specific heat of titanium is 1653 K and 580 J/kg K; and of aluminium is 890 K and 870 J/kg K, respectively [31]. The model parameters for the 4340-H steel of the FSP are taken from the study of Johnson and Cook [27].

As it was discussed in Section 2, the structure in the zone of bonding is complex and may be modelled on several levels of observations. The question should be stated if it is possible to represent accurately the bonding zone and phenomena occurred during its failure by means of simple, quantitative contact functions available in commercial FEM codes. In Table 2, some results of a numerical study are shown, in which different combinations of the tensile and shear failure stresses in the contact model were applied to simulate an impact with the velocity 650 m/s. Combinations

Table 2. Influence of the parameters of the tie-break failure criterion on the contact modelling. Images collected at different time steps present the projectile with a constant residual velocity.

$NFLS_{Ti-Al} = 1000 \text{ MPa}$ $SFLS_{Ti-Al} = 10000 \text{ MPa}$ $NFLS_{Al-Al} = 10000 \text{ MPa}$ $SFLS_{Al-Al} = 1000 \text{ MPa}$	$FLS_{Ti-Al} = 200 \text{ MPa}$ $SFLS_{Ti-Al} = 200 \text{ MPa}$ $NFLS_{Al-Al} = 200 \text{ MPa}$ $SFLS_{Al-Al} = 200 \text{ MPa}$	$NFLS_{Ti-Al} = 1000 \text{ MPa}$ $SFLS_{Ti-Al} = 700 \text{ MPa}$ $NFLS_{Al-Al} = 300 \text{ MPa}$ $SFLS_{Al-Al} = 200 \text{ MPa}$	$FLS_{Ti-Al} = 1000 \text{ MPa}$ $SFLS_{Ti-Al} = 1000 \text{ MPa}$ $NFLS_{Al-Al} = 0 \text{ MPa}$ $SFLS_{Al-Al} = 0 \text{ MPa}$
			
V rez = 240 m/s	V rez = 190 m/s	V rez = 0 m/s	V rez = 200 m/s

of stresses were chosen basing on the assumption that the bonding zone obtained due to the explosive welding has material properties comparable to the parent materials [33].

An objective was to find an optimal configuration of the contact failure stresses resulted in an acceptable mode of the delamination, the plug of a proper shape and the residual velocity close to the experimental value ($v_{rez} = 250 \text{ m/s}$). The table shows the sensitivity of the numerical model to different combinations of the failure stresses. After the plug separation from the plate, the projectile obtains a residual velocity of a constant value – the collected pictures were taken at different time steps but the residual velocity of the projectile was then constant. In the simulation, the values of the failure stresses allow to model the process but they were not physically proven. With decreasing values of the stresses for one interfaces, a delamination of this interface is more extensive. By choosing a set of the equal failure stresses, $NFLS_{Ti-Al} = SFLS_{Ti-Al} = NFLS_{Al-Al} = SFLS_{Al-Al} = 1000 \text{ MPa}$, it was assumed that both Ti-Ti and Al-Al interfaces are similarly resistant to a rupture. Debonding between the aluminiums layers of a range smaller than in the experiment was also obtained by this combination. This assumption should be verified experimentally. The contact condition, in which the failure stresses were close to the tensile and shear strengths of titanium and aluminium (the third table's column), did not result in a proper material response – the FSP was stopped inside the plate.

In Figure 4, the subsequent phases of the plate perforation are presented in the maps of equivalent plastic strain, shear stress and temperature. It may be observed that the localized shearing occurred in the titanium layer on the periphery of the FSP and it initiated a crack propagation. The highest value of the shear stress was then reached, for further steps of the process, it was lower but still the shearing was a dominant stress state.

It may be also noticed that a localized increase of temperature followed the shear bands. However, the temperature has not reached the melting point for the titanium, so basing on the applied model parameters, it cannot be claimed that the simulation confirms an adiabatic transformation of the structures. An increase of temperature is also noticeable on the interfaces between the layers but it is not sufficiently high to affect the bonding (the temperature close to 500 K). An explosively-welded bond

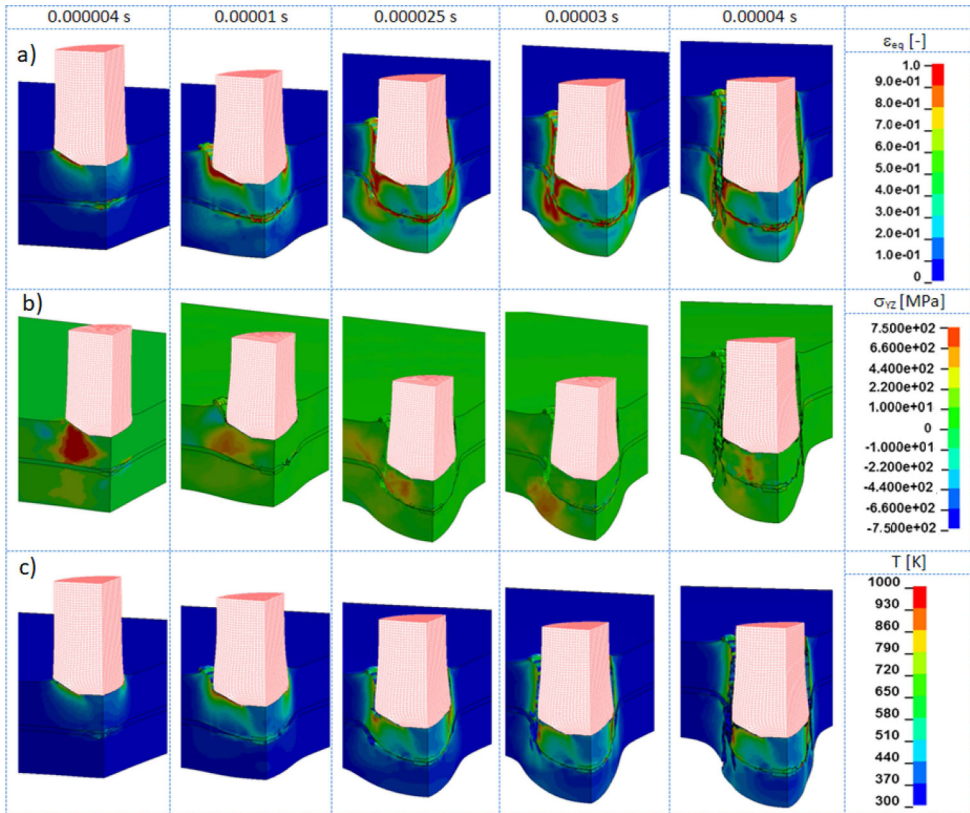


Fig. 4. Plugging of the explosive-clad plate: (a) equivalent plastic strain [-], (b) shear stress [MPa], (c) temperature [K].

has a metallurgical character and it does not result from melting of the structure of the parent materials. Similarly to them, it could be affected by a temperature close to melting. The tie-break contact function does not account for the temperature in the failure condition.

A highest decrease of the projectile velocity was calculated during the titanium perforation and it may confirm that during that stage, the largest part of the projectile kinetic energy was absorbed. A part of the titanium, which was pushed by a moving projectile, initiated the crack in the AA2519 layer (close to 0.00025 s). With the penetration going deeper, the thin AA1050 layer was highly compressed and then fracture and the backing aluminium plate expanded plastically forming a bulge. According to the simulation, the plug was separated from the plate at the final stage of the titanium perforation. The complete plug separation from the target plate is observed at 0.00004 s. At this moment, the residual velocity of the FSP decreased to 240 m/s and remained constant.

Modelling of plates welded explosively and loaded by a kinetic impact is a challenging numerical problem. Dissimilar metals joined explosively in a single plate react differently to severe deformation and a temperature increase occurred during an impact. Their plasticity and fracture should be accurately characterized. Modelling of the contact and conditions leading to its breakage is important in this type of simulations. Even if the FEM Lagrangian approach with the tie-break contact allows for modelling of an impact event with a certain accuracy, several numerical issues must be considered with caution.

5 Conclusions

Explosive welding is a technique of bonding of dissimilar metals in a layered structure providing a synergy of their physical and mechanical properties. Because layered structures are commonly used in defence applications; in this study, there are presented results of an experimental and numerical investigation performed to verify the protective performance of Ti6Al4V-AA1050-AA2519 explosively-cladded plates.

20 mm thick Ti-Al plates were impacted by fragment simulating projectiles. A monolithic 15 mm thick RHA plate with an aeral mass 118 kg/m^2 is supposed to stop a FSP accelerated to 630 m/s. The tested bi-metal plates were much lighter (the aeral mass of 73.6 kg/m^2) and due to FSPs impacts with that velocity, the target plates were perforated. To improve the effectiveness against kinetic threats, plates may be assemble together. Due to the explosive cladding, other plate thickness may be manufactured. Basing on the experimental results, the behaviour of the explosively-cladded structure under an impact loading was analysed. The FSP impacts caused a shear plugging of the tested plates. Delamination between AA1050 and AA2519 was observed. The reason of this failure was an extensive stretching of the rear, ductile AA2519 layer deformed by a moving projectile and a sheared titanium. The SEM images proved that the bonding of the layers was properly developed.

Basing on the performed impact experiments, a numerical simulation was prepared. The presented discussion on the preliminary numerical results is supposed to highlight some problems in modelling of impacts in explosively-cladded plates. The simulation requires modelling of interactions between an impactor and the subsequent target's layers and their interfaces, which behaviour and fracture is not similar. Functions describing contact provided by the FEM approach in Ls-Dyna are simplified regarding a multi-scale complexity of the joints. To obtain a more reliable modelling, the plasticity and fracture of each layer, as well as conditions of the contact rupture should be characterized.

A complex behaviour of explosively-cladded metallic laminates, especially their interfaces, is still not fully analysed. Despite lacks in the theoretical description, these structures are already applied in advanced industrial applications, mostly in the civilian and military aerospace. Experimental and numerical investigations of these metallic composites under different loadings may provide a better understanding of their properties and performance.

Manufacturing of explosively-cladded plates was supported by the National Centre for Research and Development of Poland under the Grant No. PBS/A5/35/2013. The authors would like to thank Mr. Thomas Wolf for performing the ballistic impact test and Mr. Lukasz Broda for his help with data analysis and numerical simulations.

References

1. https://en.wikipedia.org/wiki/Explosion_welding (accessed 2017/23/10)
2. B. Crossland, *Met. Mater.* **5**, 12 (1971)
3. F. Findik, *Mater. Des.* **32**, 3 (2011)
4. N. Kahraman, B. Gulenc, F. Findik, *Int. J. Impact Eng.* **34**, 8 (2007)
5. L. Qin, J. Wang, Q. Wu, X. Guo, J. Tao, *J. Alloys Compd.* **712**, 69 (2017)
6. H. Xia, W. Shao-Gang, B. Hai-Feng, *Mater. Des.* **56**, 1014 (2014)
7. D. Boronski, M. Kotyk, P. Mackowiak, L. Sniezek, *Mater. Des.* **133**, 390 (2017)
8. P. Bazarnik, B. Adamczyk-Cieslak, A. Galka, B. Plonka, L. Sniezek, M. Cantoni, M. Lewandowska, *Mater. Des.* **111**, 146 (2016)
9. I. Szachogluchowicz, L. Sniezek, V. Hutsaylyuk, *Procedia Eng.* **114**, 26 (2015)
10. I. Szachogluchowicz, L. Sniezek, V. Hutsaylyuk, *Eng. Fail. Anal.* **69**, 77 (2016)

11. A. Galka, *J. Energy Mater.* **7**, 73 (2015)
12. B. Plonka, M. Rajda, Z. Zamkotowicz, J. Zelechowski, K. Remsak, P. Korczak, W. Szymanski, L. Sniezek, *Arch. Metall. Mater.* **61**, 1 (2016)
13. S. Dey , T. Borvik, X. Teng, T. Wierzbicki, O.S. Hopperstad, *Int. J. Solids Struct.* **44**, 20 (2007)
14. E.A. Flores-Johnson, M. Saleh, L. Edwards, *Int. J. Impact Eng.* **38**, 12 (2011)
15. N. Zhou, J.X. Wang, R. Yang, G. Dong, *Theor. Appl. Fract. Mech.* **60**, 1 (2012)
16. S.A. Mousavi, S.T.S. Al-Hassani, *Mater. Des.* **29**, 1 (2008)
17. X. Wang, Y. Zheng, H. Liu, Z. Shen, Y. Hu, W. Li, Y. Gao, *Mater. Des.* **35**, 210 (2012)
18. J. Song, D. Raabe, G. Eggeler, Ph.D. thesis, Ruhr-University Bochum, 2011
19. G. Xie , Z. Luo, G. Wang, L. Li, *Mater. Trans.* **52**, 8 (2011)
20. SY. Jiang, SC. Li, L. Zhang, *Trans. Nonferrous Met. Soc. China* **23**, 3545 (2013)
21. NATO AEP-55 procedures for evaluating the protection level of logistic and light armoured vehicles, 2005, Vol. 1
22. MIL-P-46593A (NOTICE 1), Military specification: projectile, calibers .22, .30, .50, and 20mm fragment-simulating (01/06/1996) [S/S by MIL-DTL-46593B]
23. T. Fras, L. Colard, E. Lach, A. Rusinek, B. Reck, *Int. J. Impact Eng.* **86**, 336 (2015)
24. T. Fras, L. Colard, P. Pawlowski, *Int. J. Multiphys.* **9**, 3 (2015)
25. <http://www.dynasupport.com/howtos/contact/tied-tied-offset-and-tiebreak-contacts> (accessed 2017/24/10)
26. G.R. Johnson, W.H. Cook, in *Proceedings of 7th Int. Symp. on Ballistics IBS* (1983), p. 541
27. G.R. Johnson, W.H. Cook, *Eng. Fract. Mech.* **21**, 1 (1985)
28. T. Borvik, O.S. Hopperstad, T. Berstad, M. Langseth, *Eur. J. Mech. A: Solids* **20**, 5 (2001)
29. T. Fras, A. Murzyn, P. Pawlowski, *Int. J. Impact Eng.* **103**, 241 (2017)
30. V. Schulze, F. Zanger, *Procedia Eng.* **19**, 306 (2011)
31. L. Donald, Lawrence Livermore National Laboratory, FAA Report DOT/FAA/AR-00/25, IX, 2000
32. J.M.S. Morais, M.Sc. thesis, Tecnico Lisboa XI, 2014
33. D. Cutter, *Welding J.* **85** (2006)